

## CHAPTER 7

### THE EFFECT OF GeO<sub>2</sub> DOPING ON THE DIELECTRIC

### PROPERTIES OF CaCu<sub>3</sub>Ti<sub>4</sub>O<sub>12</sub> CERAMICS

#### 7.1. Introduction

Recently, much attention has been paid on CaCu<sub>3</sub>Ti<sub>4</sub>O<sub>12</sub> (CCTO) due to its high dielectric constant  $\epsilon_r \sim 10,000$  to 100,000 and fine thermal stability over a wide temperature ranges from 100-400K. The dielectric properties of CCTO make it has a potential for important applications in microelectronics [12, 17, 80]. CCTO has a cubic perovskite like structure with a lattice parameter,  $a \sim 7.393 \text{ \AA}$  [44]. It does not undergo any structural change over the same temperature range. In order to explain the origin of the high dielectric constant behavior in CCTO, many models have been proposed. The internal barrier layer capacitor (IBLC) model of Schottky barriers at the grain boundaries between semiconducting grains is widely accepted for analyzing the dielectric properties of CCTO [21, 28], including crystal structure and extrinsic phenomenon [41]. It is also reported that dielectric properties of CCTO depends on many factors such as processing and doping. There are many examples in the literature showing the effects of dopants (Zr, Fe, Co, Nb, Ni, Sc and La etc.) in CCTO-based dielectric ceramics [34-38, 73-74, 81]. Furthermore, D. Tsoutsou et al. [82] reported that dielectric constant in ZrO<sub>2</sub> thin film was improved by doping GeO<sub>2</sub>. In

this work, the effects of  $\text{GeO}_2$  doping on CCTO ceramics were studied. The CCTO ceramics were fabricated via a solid-state reaction. Properties of the obtained ceramics were investigated with the aim of improving its dielectric characteristics. Characterization of the samples was carried out using x-ray diffraction (XRD) and scanning electron microscopy (SEM). Physical properties such as, density, dielectric constant and loss tangent were also investigated.

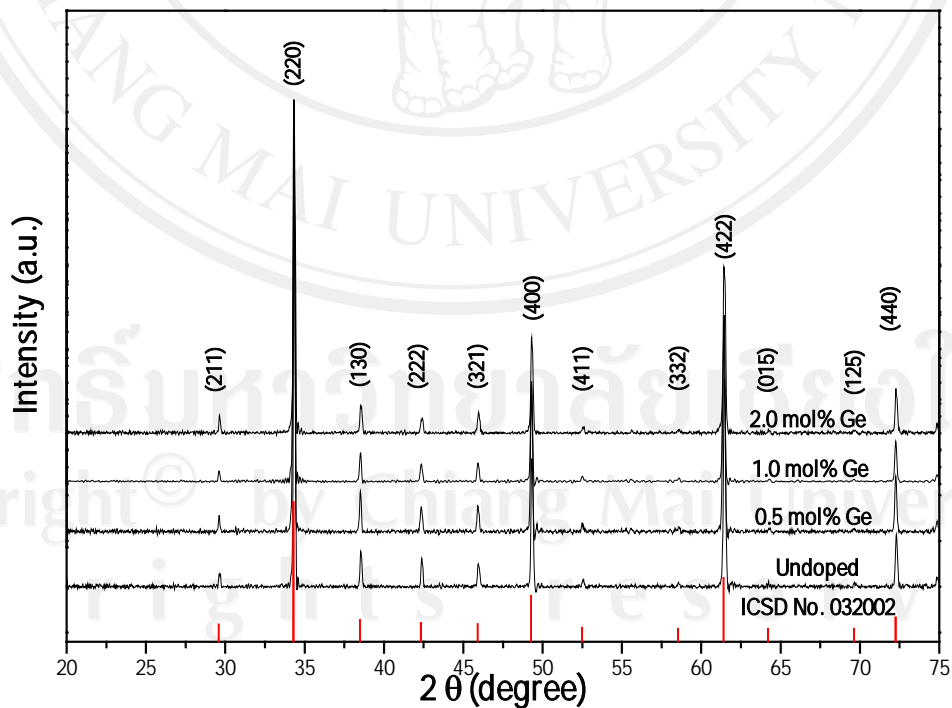
## 7.2. Experimental

The unmodified  $\text{CaCu}_3\text{Ti}_4\text{O}_{12}$  (CCTO) powder was prepared by the mixed-oxide route. High purity ( $> 99.9\%$ )  $\text{CaCO}_3$  (Riedel-de Haen),  $\text{TiO}_2$  (Riedel-de Haen) and  $\text{CuO}$  (Aldrich) powders were weighed in an appropriate ratio, fully mixed by yttria-stabilized zirconia balls in ethanol media and milled using a vibratory mill for 6 h. After being dried, the powders were calcined at  $900^\circ\text{C}$  for 2 h to form the CCTO powder. The calcined powder was granulated using polyvinyl alcohol (PVA) 3% binder and formed under a uniaxial pressure of  $2,000 \text{ kg/cm}^2$  into discs, typically 10 mm in diameter and 2 mm in thickness. The discs were sintered in air at  $1,100^\circ\text{C}$  in a step of  $5^\circ\text{C}/\text{min}$  (with soaking time of 4 h). For the doping study,  $\text{GeO}_2$  powders at various concentrations were mixed to CCTO at the calcination stage (0.5, 1 and 2 mol %). The mixtures were formed into discs employing the same process as that of the unmodified samples. The discs were sintered in air at  $1,100^\circ\text{C}$  for 4 h, with the same ramping and the cooling rates. The discs were polished to produce the flat uniform surfaces. All the samples were characterized by x-ray diffractometer (Bruker D8 Discover) at room temperature using  $\text{CuK}_\alpha$  radiation as the x-ray source. Silver paste

was used as the electrical contact. The painted samples were dried at 750 °C for 20 minutes. The polished ceramics were observed using SEM (JEOL JSM-5910LV) to study the microstructure. The dielectric constants and loss tangents against temperature were measured at the frequency of 100 Hz - 500 kHz (using Agilent 4284A LCR meter).

### 7.3. Results and discussion

The XRD patterns CCTO ceramics are displayed in Figure 7.1(A). All diffraction peaks were corresponds to the known peaks of the standard CCTO, indexed from the data in the Inorganic Crystal Structure Database (ICSD) file No.032002.



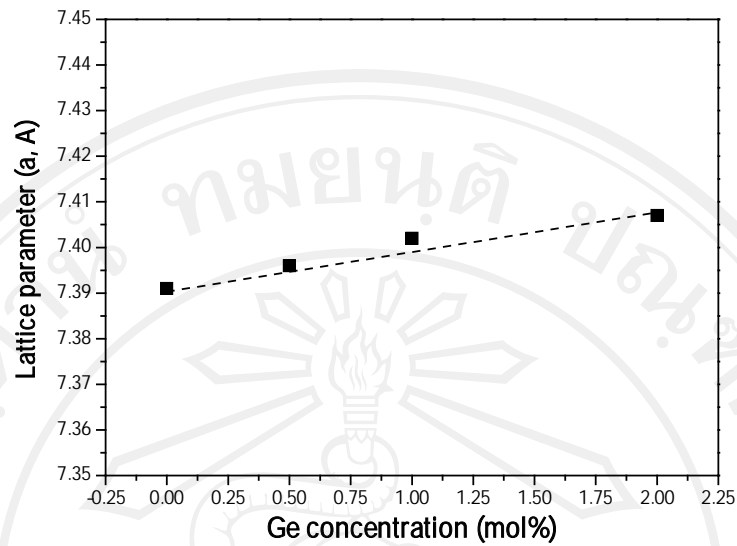


**Figure 7.1** (A) XRD patterns pure and modified CCTO: A= 0 mol% Ge, B = 0.5 mol% Ge, C = 1 mol% Ge, and D =2 mol% Ge. (B) lattice parameter (Å) as a function of Ge concentration.

All samples exhibited a phase-pure perovskite within the detection limit of the XRD equipment. The crystal symmetry of the samples at room temperature was determined to be cubic. Value of lattice constant as a function of  $\text{GeO}_2$  concentration is shown in Figure 7.1(B).

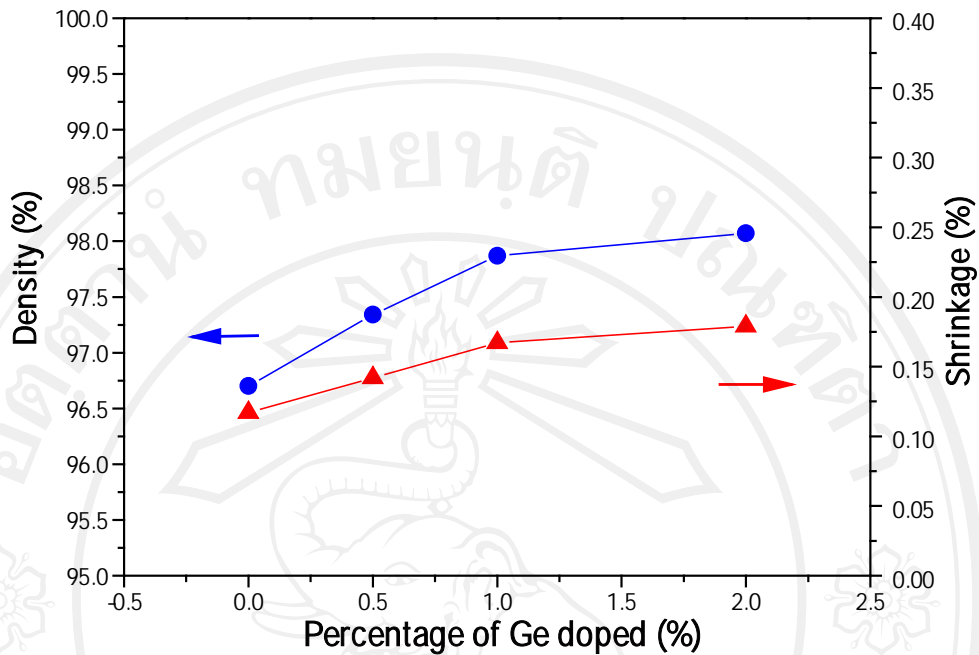
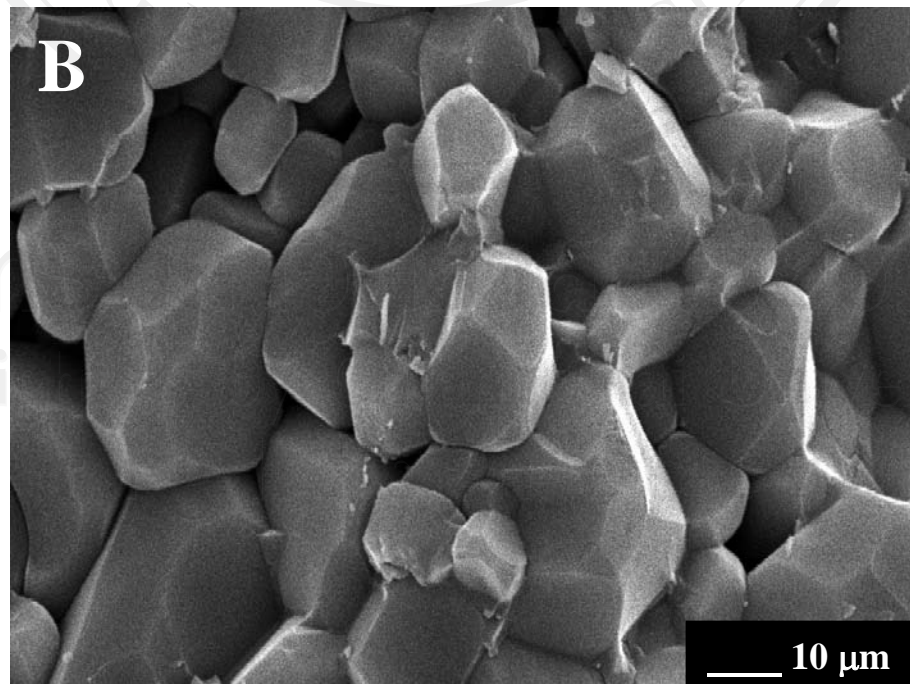
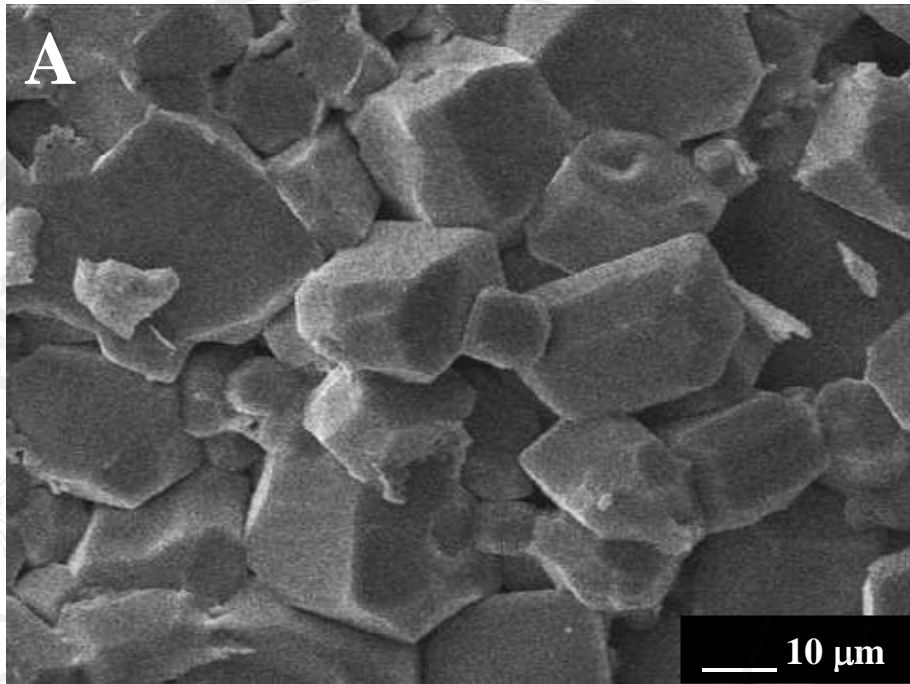


**Figure 7.2** Density and shrinkage as a function of doping concentration of the samples.

The lattice constant slightly increased with increasing the  $\text{GeO}_2$  content. In addition, the Ge doping produced a slightly improvement in the densification. The density and linear shrinkage slightly increased with increasing amounts of  $\text{GeO}_2$ . Plots of linear shrinkage and density as a function of  $\text{GeO}_2$  content are shown in Figure 7.2.

Fracture surfaces of the unmodified and doped samples are shown in Figure 7.3. Partial intergranular fracture was observed for the unmodified sample. After doping, the doped samples exhibited a non-uniform in grain size. There was some small grains occurred between large grains. The fracture mode changed to mainly

intragranular for the doped samples, suggesting a higher strengthening of the grain boundaries [83].



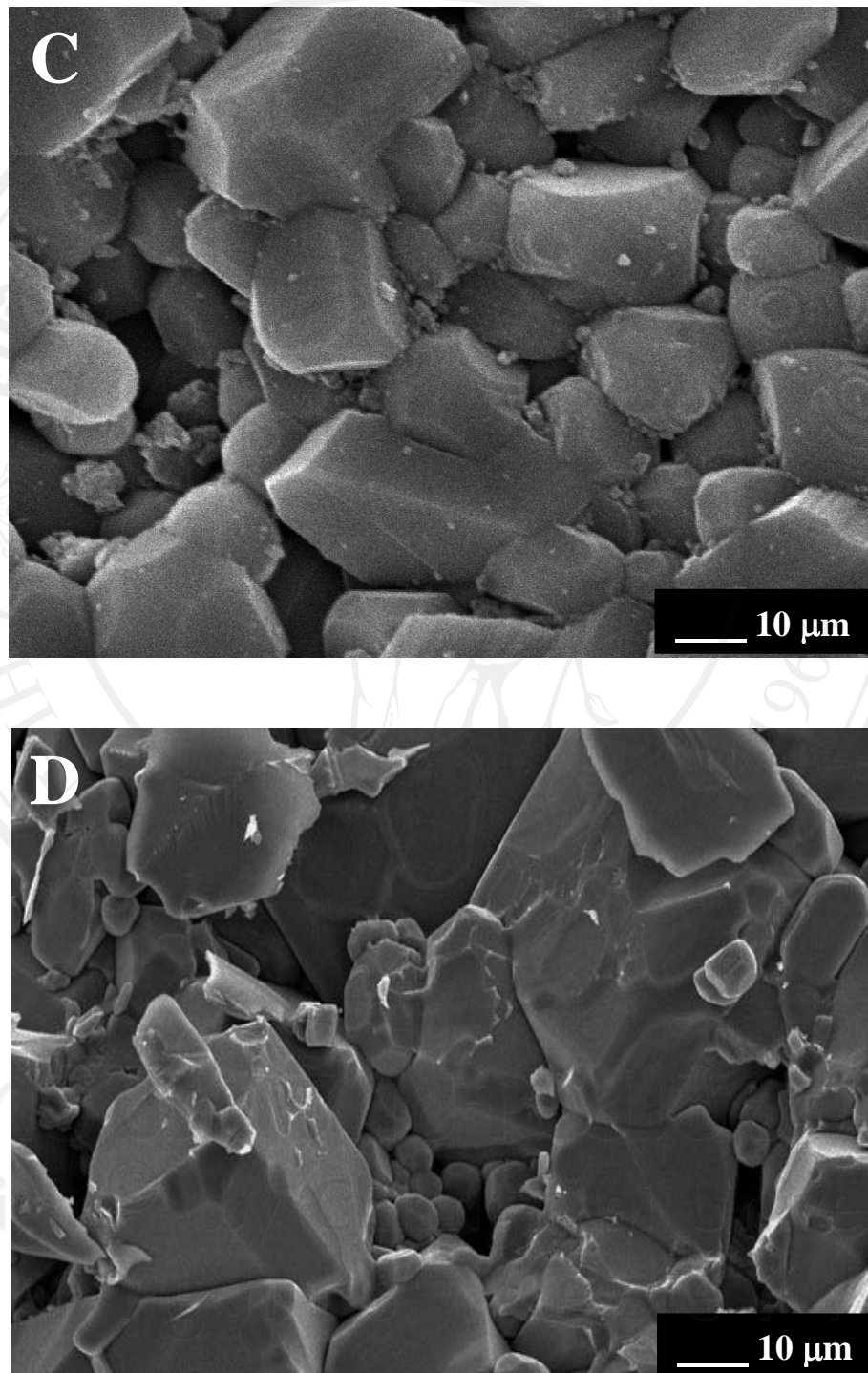


**Figure 7.3** Fracture surfaces of selected samples: (A) pure CCTO, (B) Ge 0.5

mol% doped CCTO, (C) Ge 1.0 mol% doped CCTO and

## (D) Ge 2.0 mol% doped CCTO.

These results indicate a rearrangement of grain boundary structure take place due to the effect of the addition. A slightly decrease in grain size was observed after doping: grain size slightly decreased from 20  $\mu\text{m}$  for the unmodified sample to 15  $\mu\text{m}$  for the 2.0 mol% sample. It is believed that some amount of Ge ions may go into the CCTO lattices. However, the existence of the small grains, suggested that partial Ge ions which could not go into the lattices and it produced the grain growth inhibition.

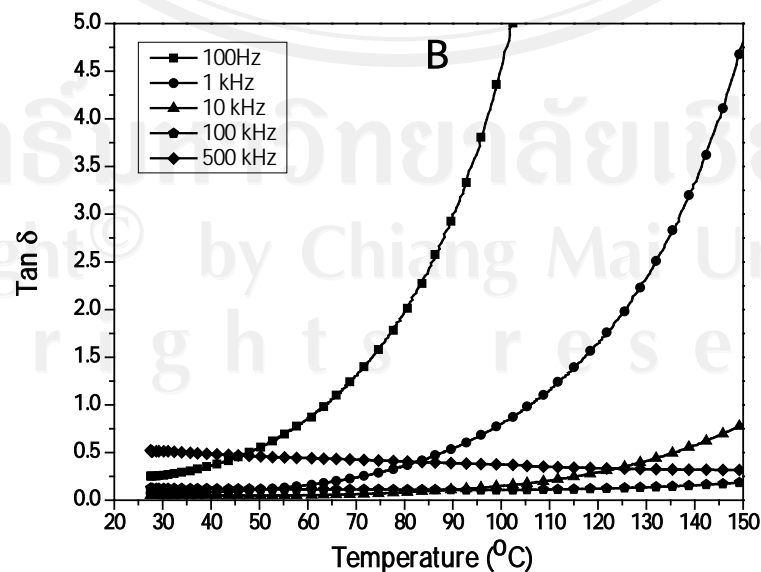
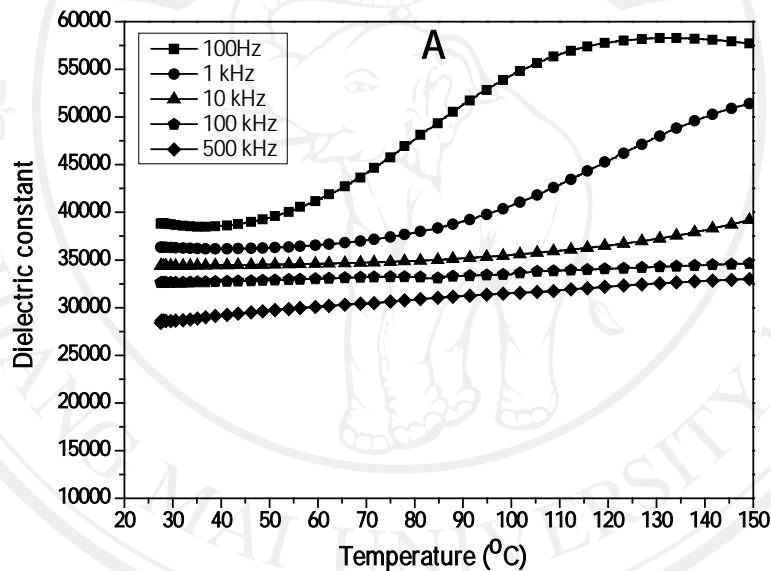
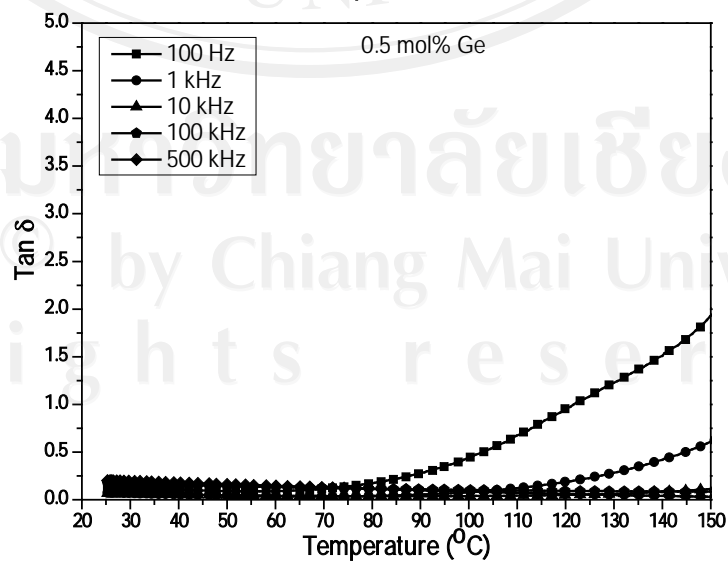
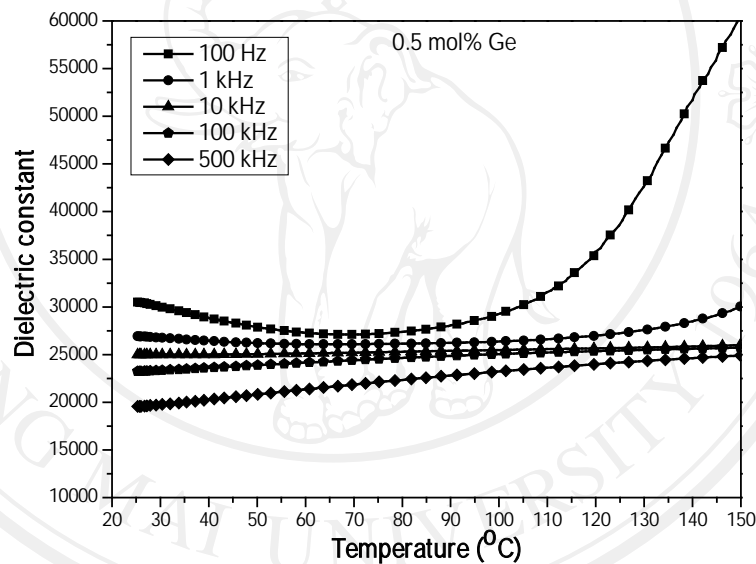


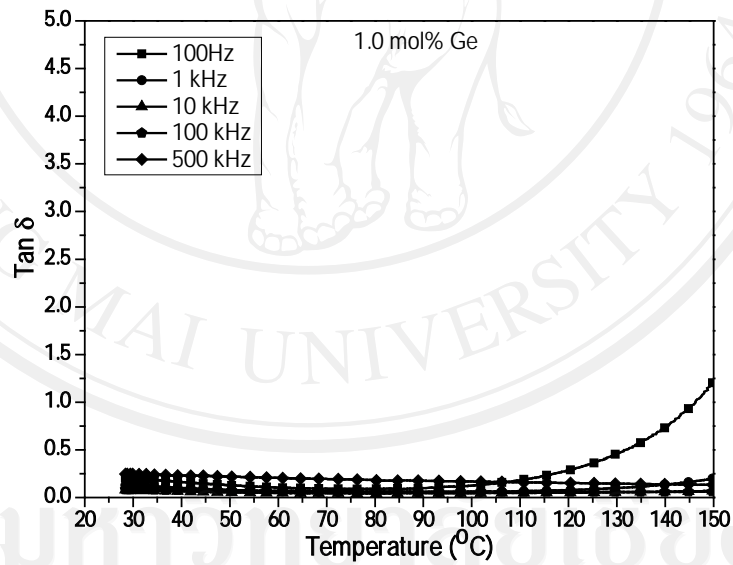
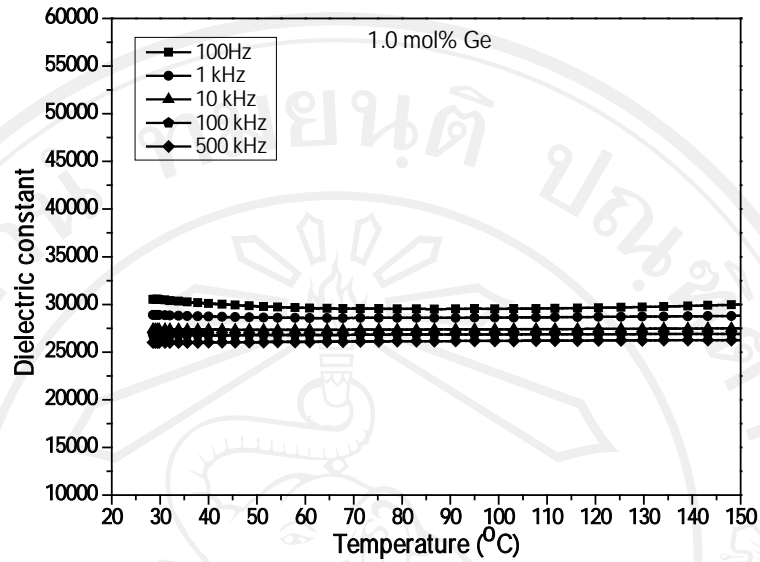
**Figure 7.4** Dielectric constant and Loss tangent as a function temperature of

the undoped CCTO samples.

The temperature and frequency dependences of dielectric constants of undoped CCTO ceramics at room temperature over the frequency range of  $10^2$ – $10^6$  Hz are illustrated in Figure 7.4. The unmodified sample showed a nearly temperature-independent at high frequencies ( $\geq 10$  kHz). The loss tangent results as seen in Figure 7.4(B), were found to consist with the dielectric results.



A



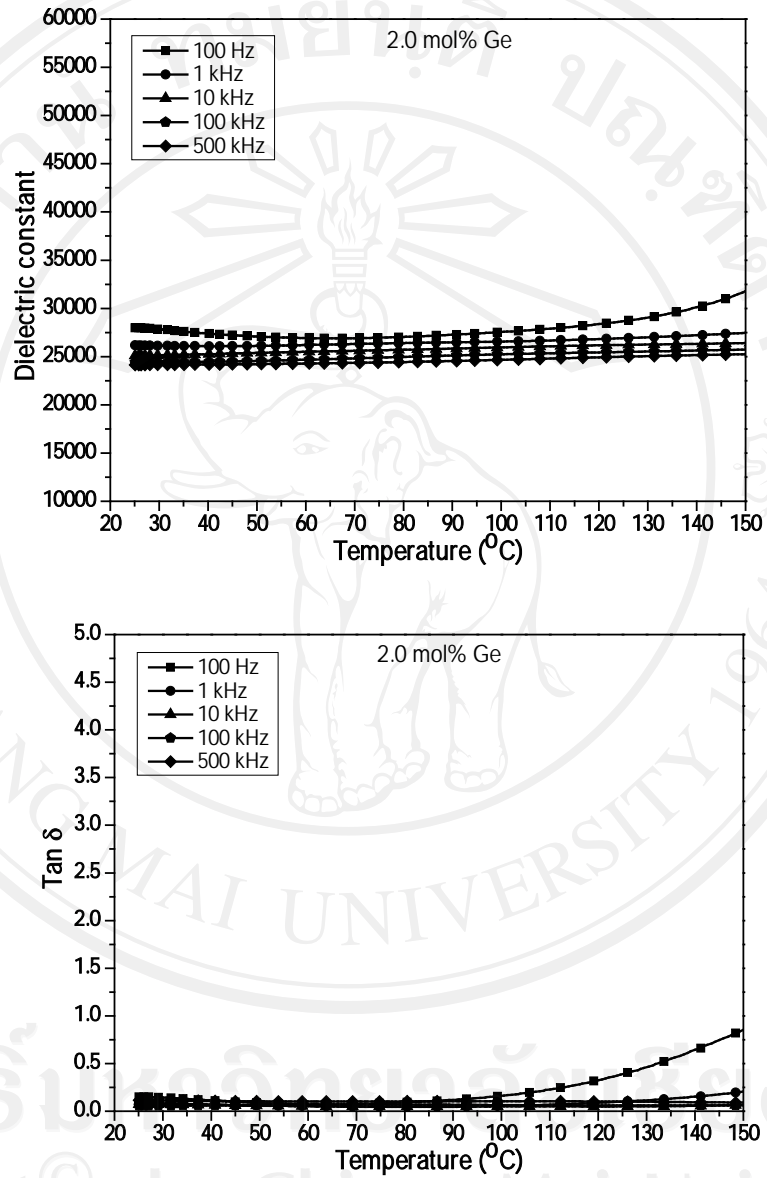
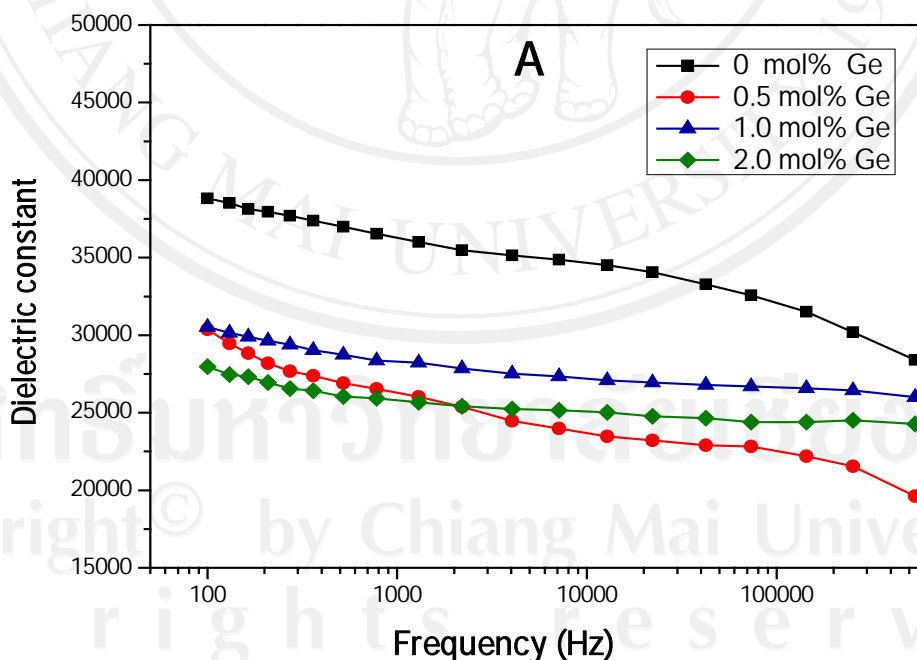


**Figure 7.5** Dielectric constant and Loss tangent as a function temperature of

the samples: (A) 0.5 mol% doped CCTO, (B) 1.0 mol% doped

CCTO and (C) 2.0 mol% doped CCTO.

Figure 7.5 shows the dielectric constant and the loss tangent as a function temperature for the doped samples. Doping  $\text{Ge}_2\text{O}_3$  produced a decrease in the dielectric constant, however, the dielectric constant still high. The 2 mol% sample had a dielectric constant  $> 26,000$  at room temperature and at 1 kHz. A nearly temperature and frequency independent of dielectric constant was observed for the doped samples (1-2 mol% samples). The loss tangent performance was also improved. A similar trend was observed for the value of loss tangent. In addition, Ge doping produced low values of loss tangent. The 2 mol% sample exhibited a lower loss tangent less than 0.08 at 1 kHz over the temperature range 25- 95 °C.



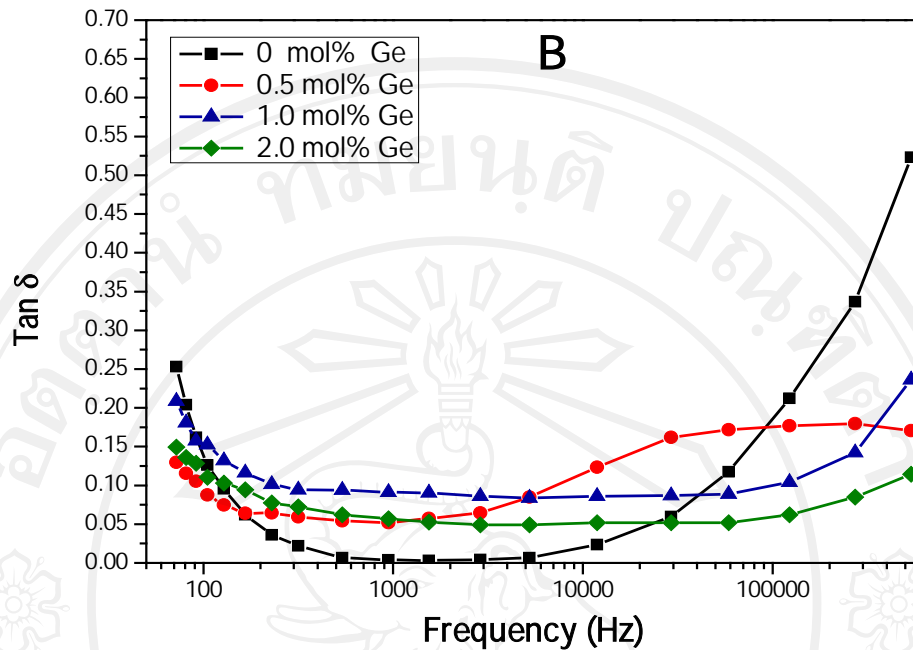


**Figure 7.6** Dielectric properties of the samples as a function of frequency:

(A) dielectric constant and (B) loss tangent.

Figure 7.6 shows dielectric constant and loss tangent as a function of frequency at room temperature. The dielectric constant decreased with frequency, but a sharp decrease was observed at the frequencies 100Hz to 1 kHz. The loss tangent decreased to a lower value with increasing frequency ( up to 1kHz) then increased with further frequency. A similar result was observed for the work done by Kwon *et al.*[57].

In this work characteristic of the grain (bulk grain and grain boundary) may be an important factor that effects on the dielectric properties of the samples. The change of the fracture mode suggested a change in grain boundary properties. It is believed that the GeO<sub>2</sub> addition produced a reduction in total resistance of the grain boundary [57]. This may cause a reduction in conductivity as a result of lower loss

tangent. Furthermore, the reduction in grain size can be associated with the decrease in dielectric constant [77, 78]. Therefore, the decrease in grain size may be a reason for the reduction of the dielectric constant for the present work. However, the microstructure of doped samples showed an existent of some small grains. In other words, the doped samples showed a large grain size distribution. Therefore, grain size distribution may be another factor to control the dielectric constant. From Figure 7.3, it should be noted that there were some cluster of small grains placed between the large gains. We believed that these small grains would have more effect on the dielectric performance than that the large grains. However, further work should be attempted to clarify this hypothesis.

#### **7.4 Conclusions**

The dielectric properties of GeO<sub>2</sub> doped CCTO was reported in this article for the first time. The doping produced a reduction in dielectric constant, but it improved the temperature and frequency stability of the dielectric constant as well as reduced the loss tangent. It is proposed that the characteristic of the grains could be responsible for the change in the properties.